PRINT ISSN 1119-8362
Electronic ISSN 2659-1502

Full-text Available Online at
https://www.ajol.info/index.php/jasem
https://www.bioline.org.br/ja

J. Appl. Sci. Environ. Manage.
Vol. 28 (2) 393-401 February 2024

Inhibition of Acid Descaling and Pickling Effects on API 5CT Carbon Steel Using Schiff Base Ligand ($C_{24}H_{21}N_5O_2$) in 1 M H_2SO_4 Solution

UGI, BU

Department of Pure & Industrial Chemistry, University of Calabar, P.M.B. 1115 Calabar, Nigeria

**Corresponding Author Email: ugibenedict@gmail.com ; Tel.: +234-7067921098*

ABSTRACT: The objective of this paper was to investigate the inhibition of acid descaling and pickling effects on API 5CT carbon steel using Schiff base ligand ($C_{24}H_{21}N_5O_2$) in 1 M H2SO4 solution using Potentiodynamic Polarization (PDP), Electrochemical Impedance Spectroscopy (EIS) and Weight Loss (WL) techniques. FTIR spectroscopy shows that there was a strong adsorption of SFBL on the carbon steel surface due to formation of a complex surface film. Corrosion rate of carbon steel decreased exceedingly from 0.0155 to 0.0002 while inhibition efficiency of SFBL rose from 78.8 % to 98.9 % between 20 ppm and 100 ppm respectively. PDP measurements revealed a mixed type inhibitor. EIS measurement reveals that the increasing charge transfer resistance was directly proportional to the increase inhibitor concentration and the double layer capacitance dropped from 1.98 to 0.61 indicating a stronger inhibition.

DOI: https://dx.doi.org/10.4314/jasem.v28i2.10

Cite this paper as: UGI, B. U. (2024). Inhibition of Acid Descaling and Pickling Effects on API 5CT Carbon Steel Using Schiff Base Ligand ($C_{24}H_{21}N_5O_2$) in 1 M H_2SO_4 Solution. *J. Appl. Sci. Environ. Manage.* 28 (2) 393-401

Dates: Received: 12 December 2023; Revised: 26 January 2024; Accepted: 10 February 2024 Published: 28 February 2024

Keywords: spectroscopy; corrosion; pickling; descaling; inhibition

Metals are widely used in today's world especially in the fields of engineering – shipping, building, construction, machining, automobile, petroleum, mining, etc (Ameh and Eddy, 2018; Ugi *et al.*, 2024). The beauty and strength experienced from this metals while in use allow for its wider application. But the wide application of metal is truncated by the damage caused by corrosion effects. These aggressiveness from corrosion could tamper with the metal's durability, tensile strength, malleability, ductility, conductivity, illustriousness, etc. Corrosion which is the deterioration of a metal under unfavorable environmental conditions (Ammouchi *et al.*, 2020; Bashir *et al.*, 2020; Ugi, 2021) has come a long way and seemed only to be managed as hopes of complete eradication of the effects is dripping off considering the different growing environmental conditions experienced today especially from greenhouse effects. The cause of corrosion is widely attributed to the chemistry involved – electro-chemical or chemical corrosion process and the processes involved in the preparation and treatment of these metals before their application, for instance during acid pickling, acidization, descaling, fracking processes, etc. (Bhuvaneswari *et al.*, 2021; Diki *et al.*, 2021). However, so much has been done in establishing an alternative means to combat corrosion effects through the deployment of chemical inhibitors. These type of inhibitors posed serious threat to the environment and the ecological system, they were expensive in production, difficult to secure (not easily assessable), and dangerous to health (Ugi and Ugi 2023). Schiff

**Corresponding Author Email: ugibenedict@gmail.com*
Tel.: +234-7067921098

base ligands which are ecologically friendly are mostly in use today in the area of corrosion mitigation. Schiff bases are usually synthesized from the condensation of primary amines and active carbonyl groups. The azomethine linkage (HC=N) and the donor atoms in the back bone of the Schiff bases are responsible for their biological and industrial applications, which can be altered depending upon the type of substituent present on the aromatic rings. Moreover, the ionic exchange between the mild steel and hetero-atoms such as O, N, P, S and double/triple bonds or aromatic rings plays an important role in the adsorption process. These group of inhibitors are opted for because they do not posed any threat to the environment and the ecological system, they are not expensive in production, easily assessable, and harmless to both man and animal health (Ebenso *et al.*, 2021; Erteeh *et al.*, 2021; Ugi *et al.*, 2021). The objective of this paper was to investigate the inhibition of acid descaling and pickling effects on API 5CT carbon steel using Schiff base ligand ($C_{24}H_{21}N_5O_2$) in 1 M H2SO4 solution.

MATERIAL AND METHODS

Preparation of Specimens: The API 5CT low carbon steel adopted for this work has the following composition by weight percentage: Si – 0.5, C – 1.5, Mn – 1.5, P – 0.022, S – 0.016 and the rest Iron. The carbon steel sheet was resized mechanically to a dimension of 5 x 4 x 0.012 cm and then polished with series of emery paper of variable grades starting with the coarsest and then proceeding in steps to the finest grade. They resized carbon steel coupons were later washed with distilled water, rinsed with absolute ethanol, dried in air after rinsing with acetone. For the electrochemical experiment, the carbon steel sheet was resized into a dimension of 1 x 1 cm and polished in preparation for the experiment using silicon carbide emery paper of different grades (400 to 1200 grit) and subsequently cleaned with acetone and rinsed with distilled water and stored. Serial dilution was used to prepare different concentrations of the Schiff base ligand inhibitor ranging from 20, 40, 60, 80 and 100 ppm.

Synthesis of Schiff base ($C_{24}H_{21}N_5O_2$): 5 g of 4-amino antipyrine at a concentration of 0.05 M was digested in a 50 ml methanolic solution of 5 g 4-(Benzeneazo) Salicylaldehyde and magnetically stirred using a 250 ml round bottom flask. This was followed by the addition of 2 ml acetic acid and refluxed for 6 hours and allowed to cool. A light green precipitate was obtained and then filtered, recrystallized with ethanol and oven dried at 60 0C. The chemical equation for the synthesis id shown in Figure 1

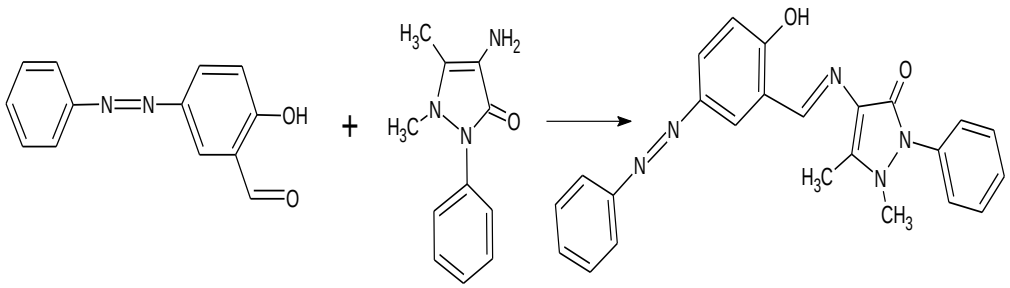

Fig. 1. Chemical equation showing the synthesis of $C_{24}H_{21}N_5O_2$*Spectroscopic and Surface Characterization:*

The UV - 2500 PC and SHIMADZU FTIR-8400 spectrophotometers were used in the study of electronic spectra of compound and structural study respectively. This study was to enable the understanding of the active compound responsible for the adsorption. The process involved the immersion of the resized carbon steel sheets in 200 ml of 1 M H_2SO_4 acid solution containing the inhibitor and allowed for 72 hours, after which they were retrieved, dried, and the films scraped and used for the surface characterization according to previous studies of Ugi and Ugi (2024) and, Bhuvaneswari (2021).

Gravimetric Technique: The gravimetric experiment was carried out using resized mirrow-polished API 5CT Carbon Steel sheets, thermostated water bath, Mettler Toledo PB602 analytical weighing balance and glass wares at concentrations of 20 ppm, 40 ppm, 60 ppm, 80 ppm and 100 ppm respectively, according to previous works of Bhuvaneswari (2021). The inhibition efficiency (IE), and degree of surface coverage (Ɵ) of mild steel in 1M HCl solution was computed using the formula as shown Equation 1 and 2 respectively.

$$\%IE = \frac{(L)o-(L)inh}{(L)o} \times 100 \quad (1)$$

Where: $(L)_o$ = corrosion rate of metal without Schiff base ligand inhibitor, $(L)_{inh}$ = corrosion rate of metal with Schiff base ligand inhibitor inclusive.

$$\theta = \frac{(L)o-(L)inh}{(L)o} \qquad (2)$$

Where all abbreviations are same as in equation 1.

Electrochemical Measurements: A computer-controlled potentiostat/galvanostat (Autolab PGSTAT 302N) consisting of saturated calomel electrode (SCE) as reference electrode (RE), platinium as counter electrode (CE) and API 5CT Carbon Steel sheets as working electrode (WE) was used. Before each potentiodynamic polarization (Tafel) study, the electrode was allowed to corrode freely and its open circuit potential (OCP) was recorded as a function of time up to 1 hour, which was sufficient to attain a stable state. Potentiodynamic polarization studies were conducted from cathodic to the anodic direction on the potential range ±250 mV versus corrosion potential (E_{corr}) at a scan rate of 10 mV/s. Linear polarization resistance measurements (LPR) were carried out at the potential range ±20 mV with respect to the open circuit potential, and the current response was measured at a scan rate of 0.5 mV/s. The EIS measurements were performed once the OCP was stabilized at a frequency range of 100 KHz to 10 MHz with a signal amplitude perturbation of 5 mV. The inhibition efficiency (%) from PDP was calculated from the measured I_{corr} values using equation 3.

$$I(\%) = \left(\frac{A^o_{corr} - A_{corr}}{A^o_{corr}}\right) \times 100 \qquad (3)$$

Where A^o_{corr} = corrosion current densities in the absence of Schiff base ligand; A_{corr} = are the corrosion current densities in the presence of Schiff base ligand;

The polarization resistance was obtained using the Stern-Geary equation 4.

$$R_p = \frac{G_a \times G_c}{2.303 \times l_{corr} \times (G_a + G_c)} \qquad (4)$$

Where G_a and G_c are the anodic and cathodic Tafel slopes. From the measured R_p values, the inhibition efficiency (%) was calculated using Equation 5.

$$I(\%) = \left(\frac{R_p - R^o_p}{R_p}\right) \times 100 \qquad (5)$$

where R^o_p and R_p are the polarization resistance values in the absence and presence of inhibitors.
The constant phase element which is defined by *Yo* and *n* has correlation with the impedance as follows equation 6

$$ZZ_{CPE} = Y_o^{-1}(j\omega)^{-n} \qquad (6)$$

where Y_o is the CPE constant and *n* is the CPE exponent, j= $(-1)^{½}$ which is an imaginary number and ω is the angular frequency in rad/s. The double layer capacitance (C_{dl}) values were calculated from equation 7 expression.

$$C_{dl} = \frac{1}{\omega R_{ct}} = \frac{1}{(2\pi f_{max} R_{ct})} \qquad (7)$$

Where ω is the angular frequency ($\omega = 2\pi f_{max}$), f_{max} is the frequency at which the imaginary component of the impedance is maximum. The inhibition efficiency acquired from the impedance spectroscopy measurements were calculated using equation 8:

$$\%IE = \frac{U_{ct(inh)} - U^o_{ct}}{U_{ct(inh)}} \times 100 \qquad (8)$$

Where $U_{ct(inh)}$ and U^o_{ct} are the charge transfer resistance in the presence and absence of inhibitor, respectively.

RESULTS AND DISCUSSION

Electronic spectra of the Schiff base ligands: SBL2 showed three essential absorption bands at 248.4 nm (40081.16 cm-1), 274.1 nm (36362.54 cm-1) and 321.4 nm (31200.23 cm-1). The band appearing at lower energy (248.4 and 274.1 nm) was indicative of a n – π* transition due the nonbonding electrons present on the nitrogen atom of the -HC=N group and the phenolic group. The band observed at higher energy (321.4 nm) was consequent of π – π* transition of the ligand centered transitions of benzene ring (Fouda *et al.*, 2021; Liu *et al*., 2020; Haruna and Saleh, 2022).

FT-IR spectral analysis: Peaks attributable to the functional groups were shown from the observed infrared spectra. The efficacy of the Schiff base to adsorb strongly on the carbon steel was evident by the presence of the identified functional groups. The spectra of the SFBL as well as corrosion products from the inhibitor films on the carbon steel surface are presented in Figures 2-3. Table 1 represent data generated from the infrared absorption spectra SFBL and their corrosion products. From Table 1, the C=N at 1580 and 1618 cm-1 was shifted to 1625 and 1595 cm-1, C–O stretch at 1327 cm−1was shifted to 1329 and 1364 cm−1, C–C bend at 835 cm−1 was shifted to 880 and 828 cm−1, C–C stretch at 1439 and 1416 cm−1was shifted to 1424 and 1491 cm−1, C-H stretch at 2097 and 2937 cm-1 was shifted to 2922 and 2072 cm-1 , C-N stretch at 1088 and 1081 cm-1 was shifted to 1096 cm-1and O–H stretch at 3250 and 3370 cm-1 was shifted to 3161 and 3116 cm−1. The shifts in

frequencies indicated that there was an interaction between the mild steel surface and the Schiff bases (Fouda *et al.,* 2021; Liu *et al*., 2020). On the other hand, C=C stretch at 1505.80 cm-1, C-H stretch at 2065 cm-1 and the C-H bend in the region 999 - 917 cm-1 were missing in the spectrum of the corrosion products suggesting that these functional groups were used for the adsorption of the inhibitor onto the surface of the carbon steel. This also indicated that some new bonds were also formed through these functional groups (Haruna and Saleh, 2022). Hence, protection of metallic surface was done via the functional groups presented in the inhibitor.

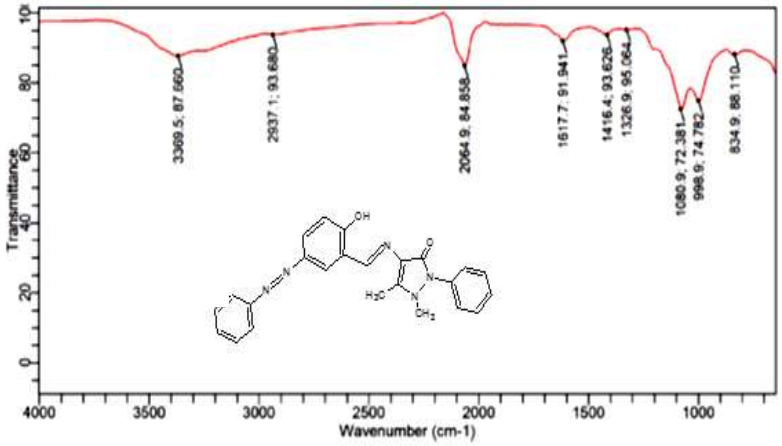

Fig. 2. FTIR spectra of SFBL

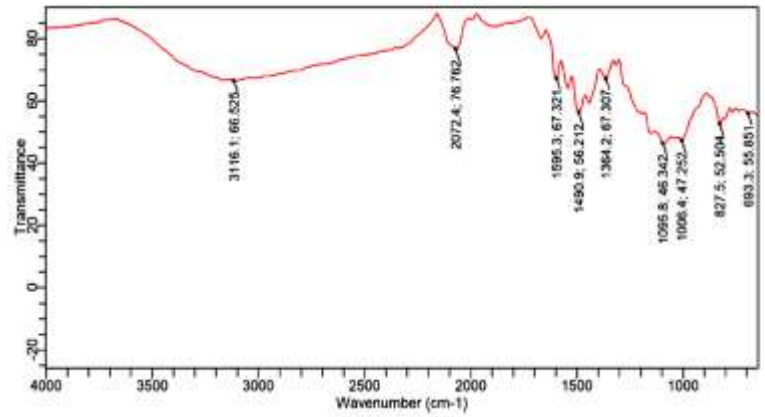

Fig. 3. FTIR spectra of the corrosion product of API 5CT carbon steel in 1 M H_2SO_4 in the presence of Schiff base ligand

Table 1. The Relevant Infrared Spectra Data for the Schiff base Ligands cm^{-1}

Compound	C-H	C--C	C-O	C-N	C=N	O-H	C-H bend
SFBL	2937	1416	1327	1081	1618	3370	835
SFBL = CS	2072	1491	1364	1096	1595	3116	828

Weight Loss Measurements: The Schiff base ligand demonstrated high adsorption tendency on the API 5CT carbon steel surface which was expressed in the high inhibition efficiency of the inhibitor (98.9 %) and decreased corrosion rate of the metal (0.0002 (gcm-2 hrs-1) x 10-2) as displayed in Table 2. This behaviour is always attributed to direct proportionality between increase inhibitor concentration and surface coverage (Ugi *et al.,* 2024; Majda *et al.,* 2020; Onyeachu *et al.,* 2021). It could also be due to, the high molecular weight and the presence of abundant electron donation groups (C=N, O-H, C-N, N=N and aromatic rings). Since corrosion is an anodic site dissolution, a consequence of oxidation at the electrode, the increased inhibition efficiency with direct increase in inhibitor concentration implies that the corrosion active sites where the anions (SO_4^{2-}) are concentrated were strongly inhibited from oxidation (Ugi *et al.,* 2024; Majda *et al.,* 2020; Onyeachu *et al.,* 2021). Hence there was no possibility of sulphtate ions which pair up to form sulphate gas, that speed up corrosion activities on the API 5CT carbon steel surface.

Table 2 Deduced data for corrosion rate and inhibition efficiency obtained from gravimetric method for API 5CT carbon steel in 1 M H_2SO_4

Concentration (ppm)	Weight Loss (g)	Corrosion Rate (gcm^{-2} hrs^{-1}) x 10^{-2}	Inhibition Efficiency (%)
Blank	0.0155	0.189	-
20	0.0033	0.040	78.8
40	0.0021	0.026	86.2
60	0.0011	0.013	93.1
80	0.0009	0.011	94.2
100	0.0002	0.002	98.9

PDP Measurements: The Tafel slope for the API 5CT carbon steel in 1 M H_2SO_4 solution and varying concentrations of Schiff base where PDP parameters were calculated out of is presented in Fig. 4. The possible equation showing the anodic oxidation of iron in the API 5CT carbon steel due to chloride effect and that of the cathode reduction are shown in Equations 9-10 (Uwah *et al.*, 2012; Padash *et al.*, 2020).

$$Fe_{(s)} \rightarrow Fe^{2+}_{(aq)} + 2e^{-} \quad (9)$$

$$2H^{+}_{(aq)} + 2e^{-} \rightarrow H_{2(g)} \quad (10)$$

From Table 3, it was observed that the corrosion current density (A_{corr}) values decreased with an increase in inhibitor concentration compared to the free acid solution. This is due to formation of adsorbed protective film of the Schiff bases on API 5CT carbon steel surface (Rbaa *et al.*, 2020; Sharma *et al.*, 2021; Ugi *et al.*, 2022). The Ecorr values obtained from the analysis suggest that the Schiff base inhibitor have dominant influence on the partial anodic and cathodic reaction. The addition of the Schiff base inhibitor further shifted the corrosion potential (E_{corr}) towards negative values much less than - 85 mV/SCE, hence acted as a mixed type inhibitor (Ebenso *et al.*, 2021). The values of Gc and Ga obtained change on addition of inhibitor from that of the free acid solution (Table 3.). The calculated inhibition efficiency also increased with an increase in concentration of the inhibitor, similar to EIS results. The values of polarization resistance were observed to increase with corresponding increase in inhibition efficiency of the inhibitor as shown in Table 3. This result is in conformity with those of potentiodynamic polarization and electrochemical impedance spectroscopy. This phenomena is always in tandem with the theory of strong inhibitor molecular adsorption on surface of the API 5CT carbon steel (Ameh and eddy 2018; Ugi *et al.*, 2024).

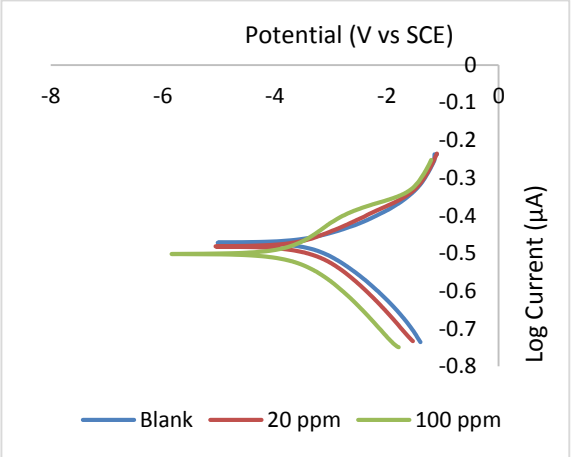

Fig. 4. Tafel plots for mild steel corrosion in 1 M H_2SO_4 containing different concentrations of Schiff base ligand.

Table 3. PDP parameters for API 5CT carbon steel in 1 M H_2SO_4 in the absent and presence of SFBL

Concentration (ppm)	- E_{corr}(mV)	A_{corr} (µA)	G_c(V/dec)	G_a(V/dec)	η%	R_p (Ωcm^2) x 10^{-2}	η%
Blank	510	116	114.01	107.11	-	1.009	-
20	542	519	133.07	126.85	77.65	5.004	79.84
100	574	997	169.29	199.72	88.37	9.208	89.04

EIS Measurement: In order to access the inhibitor (Schiff bases) viability in creating a resistance on charge transfer between the working electrode and solution, the Nyquist plot as shown in Figure 5 was obtained. The various data calculated from the plots are presented in Table 4. From the Nyquist plots, it was observed that the diameter of the semicircles obtained were influences by both the free acid and the various concentrations of the Schiff base inhibitor. The difference in sizes of their diameters could be attributed to the strong adsorption of the Schiff base on the working electrode (API 5CT carbon steel), hence increasing the charge transfer resistance (U_{ct}) at the working electrode and decreasing the solution resistance (Rs) of the electrolyte as concentration of the inhibitor increases (Agwamba *et al.*, 2022; Ugi *et al.*, 2025; 2020; Nya *et al.*, 2018). However, the addition of SFBL further increased the diameter of the capacitive loop (Figure 5). The EIS plots were noticed to show some level of imperfection and a single capacity loop and could be linked to API 5CT carbon steel surface roughness, noise effects and a charge transfer type (process) of mechanism of inhibition (Agwamba *et al.*, 2022; Ugi *et al.*, 2025; 2020; Nya *et al.*, 2018). The degree of roughness or non-homogeneity (n1) of API 5CT carbon steel was found to decreased on addition of SFBL, suggesting that the surface roughness of the steel was decreased on

adsorption of inhibitor molecules on steel surface active sites and this result is in agreement with those of the morphology (SEM) test (Ugi and Magu 2012; Tan *et al.,* 2020). A decrease in n on addition of inhibitors also signified insulation of the metal/solution interface by formation of a surface film. Formation of this film resulted in increase in charge transfer resistance in the presence than in the absence of inhibitor. The inhibition efficiency obtained also increased with increase in inhibitor concentration, hence consistent with weight loss results. The C_{dl} values decreased in the presence of inhibitors and could be attributed to a decrease in the local dielectric constant or increase in the thickness of the double layer or both, caused by the adsorbed protective film of the inhibitors as earlier inferred (Su *et al.,* 2020; Ugi 2014; Uwah *et al*., 2013; Ugi *et al*., 2016).

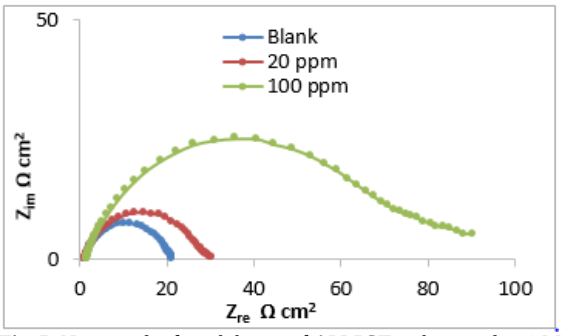

Fig. 5. Nyquist plot for inhibition of API 5CT carbon steel in 1 M H_2SO_4 in the absence and presence of SFBL

Table 4. EIS parameters for API 5CT carbon steel in 1 M H_2SO_4 containing different concentrations of SFBL

EIS Parameters	1 M H_2SO_4	20 ppm	100 ppm
U_{ct} (Ωcm^2)	18.9	39.4	99.3
R_s (Ωcm^2)	1.34	1.30	1.16
χ^2 x 10^{-4}	7.96	0.77	0.20
$Y_{o1}(\Omega s^n cm^{-2})$ x 10^{-4}	2.26	1.46	1.00
n_1 x 10^{-1}	8.53	8.18	7.97
R_f (Ωcm^2)	4.20	0.42	0.74
$Y_{o2}(\Omega s^n cm^{-2})$ x 10^{-2}	5.31	4.17	0.83
n_2 x 10^{-1}	1.87	0.84	0.50
C_{dl} (μF) x 10^{-2}	8.14	0.78	0.65
Ƞ%	-	52.03	80.97

Adsorption Isotherm: In order to understand the nature of adsorption whether physical (mono layer) or chemical and to further investigate the molecular interaction of the inhibitor while on the metal surface, the Langmuir and Frumkin adoption isotherms were used. The Langmuir adsorption isotherm was deduced for the plot of $\frac{C}{\theta}$ vs C using equation 11 (Zaher *et al.,* 2020; Ebenso *et al.,* 2021; Ugi and Abeng 2013; Ugi *et al*., 2016).

$$\frac{C}{\theta} = \frac{1}{K} + C \qquad (11)$$

Where C is the inhibitor concentration and K the binding constant of corrosion inhibition process.

Of greater significance in applying the Frumkin adsorption isotherm is the molecular interactive parameter 'a'. This parameter establishes the strength of attractive forces binding the Schiff base molecule to the API 5CT carbon steel surface and the parameter can either be negative or positive in action. Positive or negative values suggest strong attraction or repulsive (weak) forces between adsorbed molecules respectively (Ugi *et al.,* 2019; Ugi 2021; Su *et al.,* 2020; Joshi *et al.,* 2021). This molecular interaction parameter was determined from the slope of the plot of surface coverage, θ vs. log C (g/L) according to the Frumkin Equation 12.

$$\ln\left(\left(\frac{\theta}{1-\theta}\right)/C\right) = lnKads + 2a\theta \qquad (12)$$

Where, θ is surface coverage, '*a*' is interaction parameter, K_{ads} is the equilibrium constant and C is the Schiff base concentration.

From Table 5, it can be deduced that the data from the interaction between the Schiff base ligand and the API 5CT carbon steel surface fitted very well to the Langmuir than the Frumkin isotherm considering their correlation coefficient values. The Langmuir correlation values were 0.99 across the various temperatures which implies that the inhibition process was a physically adsorbed one and connotes a monolayer adsorption process (Ugi 2024; Nya *et al.,* 2018; Ammouchi *et al.,* 2020). From the Frumkin adsorption data, the interaction parameter values were all positive implying that there was a strong inhibitor molecular interaction between the Schiff base and the carbon steel. The values of the binding coefficient decreased while temperature was increased. This follows the possible desorption of Schiff base molecules from the API 5CT carbon steel surface at higher temperatures due to strong heat agitation of surface interaction.

Table 5. Langmuir and Frumkin adsorption isotherm data for API 5CT carbon steel in 1 M H_2SO_4 solution

	Langmuir				Frumkin			
Temp. (K)	K_{ads}	R^2	Slope	ΔG^*_{ads} (kJ/mol)	K_{ads}	a	R^2	ΔG^*_{ads} (kJ/mol)
303	23.87	0.9993	1.06	-4.442	2.23	4.31	0.8571	-13.34
313	9.06	0.9959	1.12	-3.184	1.92	4.78	0.8571	-12.15
333	3.04	0.9514	1.18	-1.713	1.92	4.78	0.8865	-11.76

This result alongside those of the adsorption free energy (ΔG^*_{ads} (kJ/mol) showing values < -40 kJmol^{-1} explains a physical adsorption mechanism and stronger inhibition at lower temperatures (Nya *et al.*, 2018; Ammouchi *et al.*, 2020

Conclusion: The various experimental results affirmed the synthesized Schiff base ligand ($C_{24}H_{21}N_5O_2$) to be very effective in the corrosion inhibition arising from H2SO4 acid descaling and pickling effects on API 5CT Carbon Steel. Inhibition was confirmed to be through strong inhibitor molecular adsorption by a physical adsorption mechanism. The Schiff base ligand provided a stabled inhibitor - API 5CT carbon steel surface adsorption, spontaneous reaction, strong molecular interaction and mono layer adsorption.

Conflicts of Interest: Authors clearly state that there is no any personal circumstances or interests that may be identified as inappropriately affecting the representation or explanation of reported research results.

REFERENCES

Agwamba, EC; Udoikono, AD; Hitler, L (2022). Synthesis, characterization, DFT studies, and molecular modeling of azo dye derivatives as potential candidate for trypanosomiasis treatment. *Chem. Phys. Impact*., 4: 100076. http://doi.org./10.1016/chphi.2022.100076

Ameh, PO; Eddy, NO (2018). Experimental and computational chemistry studies on the inhibition efficiency of phthalic acid (PHA) for the corrosion of aluminum in hydrochloric and tetraoxosulphate (VI) acids. *Prot. Metals Phys. Chem. Surf.*, 2: 1-13. http://doi.org./10.1134/S2070205118060035

Ammouchi, N; Allal, H; Belhocine, Y (2020). DFT computations and molecular dynamics investigations on conformers of some pyrazinamide derivatives as corrosion inhibitors for aluminum. *J. Mol. Liq*., 300: 112309. http://doi.org./10.1016/j.molliq.2019.112309

Bashir, S; Sharma, V; Kumar, S (2020). Inhibition performances of Nicotinamide against aluminum corrosion in an acidic medium. *Portugal. Electrochim. Acta.*, 38: 107-123. http://doi.org./10.4152/pea.202002107

Bhuvaneswari, M; Santhakumari, R; Usha, C (2021). Synthesis, growth, structural, Spectroscopic, optical, Thermal, DFT, HOMO–LUMO, MEP, NBO analysis, and Thermodynamic properties of vanillin isonicotinic hydrazide single crystal. *J. Mol. Struc*., 4: 130856. http://doi.org./10.1016/j.molstruc.2021.130856

Diki, NYS; Coulibaly, NH; Kambire, O (2021). Experimental and theoretical investigations on copper corrosion inhibition by cefixime drug in 1 M HNO_3 solution. *J. Mater. Sci. Chem. Engr*., 9: 212. http://doi.org./10.4236/msce.2021.95002

Ebenso, EE; Verma, C; Olasunkanmi, LO (2021). Molecular modelling of compounds used for corrosion inhibition studies: a review. *Phys. Chem. Chem. Phys.*, 23: 19987 – 20027. http://doi.org./10.1039/D1CP00244A

Erteeb, MA; Ali-Shattle, EE; Khalil, SM (2021). Computationl studies (DFT) and PM3 theories on thiophene oligomers as corrosion inhibitors for iron. *American J. Chem.*, 11: 1 – 7. http://doi.org./10.5923/j.chemistry.20211101.01

Fouda, AE; El-Askalany, AH; Molouk, AFS (2021). Experimental and computational chemical studies on the corrosion inhibitive properties of carbonitrile compounds for carbon steel in aqueous solution. *Sci. Rep.* 11: 67 – 79. http://doi.org./10.1038/s41598-021-00701-z

Joshi, BD; Thakur, G; Chaudhary, MK (2021). Molecular structure, homo-lumo and vibrational analysis of ergoline by density functional theory. *Science World*, 14: 21–30. http://doi.org./10.3126/sw.v14i14.34978

Liu, Q; Song, Z; Han, H (2020). A novel green reinforcement corrosion inhibitor extracted from waste Platanus acerifolia leaves. *Construc. Build. Mater.*, 260: 119695. http://doi.org./10.1016/j.conbuildmat.2020.119695

Majda, MT; Ramezanzadeh, M; Ramezanzadeh, B (2020). Production of an environmentally stable anti-corrosion film based on Esfand seed extract molecules- metal cations: Integrated experimental and computer modeling approaches. *J. Hazard. Mater.*, 382: 1-16. http://doi.org./10.1016/j.hazmat.20192019.12102

Nya, NE; Okafor, PC; Ikeuba, AI; Ugi, BU (2018), Mild steel corrosion mitigation in Sulphuric acid via benign isolated phytochemicals from Viscum album. *J.Mater. Sci. Chem. Engr*., 6: 132 – 146

Onyeachu, IB; Abdel-Azeim, S; Chauhan, DS (2021). Electrochemical and Computational insights on the application of expired Metformin drug as a novel inhibitor for the sweet corrosion of C1018 steel. *ACS Omega*. 6: 65 – 76. http://doi.org./10.1021/acsomega.0c03364

Padash, R; Sajadi, GS; Jafari, AH (2020). Corrosion control of aluminum in the solutions of NaCl, HCl and NaOH using 2, 6-dimethylpyridine inhibitor: Experimental and DFT insights. *Mater. Chem. Phys..*, 244: 122681. http://doi.org./10.1016/j.matchemphys.202012681

Rbaa, M; Ouakki, M; Galai, M (2020). Simple preparation and characterization of novel 8-Hydroxyquinoline derivatives as effective acid corrosion inhibitor for mild steel: Experimental and theoretical studies. *Col. Surf. A: Phys. Engr. Aspect.*, 602: 125094. http://doi.org./10.1016/j.colsurfa.2020.125094

Sharma, S; Ganjoo, R; Saha, SK (2021). Experimental and theoretical analysis of baclofen as a potential corrosion inhibitor for mild steel surface in HCl medium. *J. Adhes. Sci. Tech..*, 1: 119. https://doi.org/10.1080/01694243.2021.200230

Su, P; Li, L; Li, W (2020). Expired drug theophylline as potential corrosion inhibitor for 7075 aluminum alloy in 1M NaOH solution. *Int. J. Electrochem. Sci.*, 15: 1412 – 1425. http://doi.org./10.20964/2020.02.25

Tan, J; Guo, L; Wu, D (2020). Electrochemical and computational studies on the corrosion inhibition of mild steel by 1-Hexadecyl-3-methylimidazolium Bromide in HCl medium. *Int. J. Electrochem. Sci.*, 15: 1893 – 1903. http://doi.org./10.20964/2020.03.36

Ugi, BU (2024). DFT and Electrochemical Study of Novel Green Corrosion Inhibitor (Pyrantrin) for 1100-H14 Aluminum Corrosion Remediation in 1 M H2SO4 Acidic Environment. J. Turkish Chem. Soc. A: Chem. 11(1): 253 -260

Ugi, BU (2014). Alkaloid and Non Alkaloid Extracts of *Solanum melongena* Leaves as Green Corrosion Inhibitors on Carbon Steel in Alkaline Medium. *Fountain J. Nat. Appl. Sci.* 3(1): 1 – 9

Ugi, BU (2021) Corrosion Inhibition of Cu-Zn-Fe Alloy in Hydrochloric Acid Medium by Crude Ethanol Extracts from Roots-Leaves Synergy of *Solanum melongena. Earthline J. Chem. Sci*., 5(1) 105 – 118

Ugi, BU; Bassey, VM; Obeten, ME; Adalikwu, SA; Nandi, DO (2020). Secondary Plant Metabolites of Natural Product Origin - Strongylodon macrobotrys as Pitting Cor-rosion Inhibitors of Steel around Heavy Salt De-posits in Gabu, Nigeria. *J. Mater. Sci. Chem. Engr.* 8(5): 38 – 60

Ugi, BU; BoEkom, EJ; Ashishie, PB; Ubua, PU (2025). Scopolamine Alkaloid as Novel Green Inhibitor ofv malleable Fe Corosion Studies by EIS, DFT, PDP and SEM Techniques. *Portugal. Electrochim. Acta*. 43: 23-35. https://doi.org/10.4152/pea.20254301014

Ugi, BU; Abeng, FE (2013). Corrosion Inhibition Effects and Adsorption Characteristics of Ethanol Extract of King Bitters Root (Andrographispaniculata) on Mild Steel in 1.0 M HCl and H_2SO_4 Acid Media. *Fountain J. Nat. Appl. Sci.*, 2(2):10 – 21

Ugi, BU; Abeng, FE; Obeten, ME; Uwah, IE (2019). Management of Aqueous Corrosion of Federated Mild Steel (Local Constructional Steel) at Elevated Temperatures Employing Environmentally Friendly Inhibitors: *Matricaria chamomilla* Plant. *Int. J. Chem. Sci.*, 3(1): 6 – 12

Ugi, BU; Bassey, VM; Ashishi, PB; Nandi, DO; Ugi, FB (2024). S275JR Mild Steel Corrosion Sites Deactivation in Sodium Sesquicarbonate Heavy Deposits Using Piperaquine as Alternative Inhibitor. *Portugal. Electrochim. Acta.*, 42: 101-114. https://doi.org/10.4152/pea.2023420202

Ugi, BU; Magu, TO (2017). Inhibition, Adsorption and Thermodynamic Investigation of Iron Corrosion by Green Inhibitors in Acidic Medium. *The Int. J. Sci. Technoledge* 5(4): 56 – 64

Ugi, BU; Obeten, M; Bassey, VM; BoEkom, JB; Omaliko, EC (2021) Quantum and electrochemical studies of corrosion inhibition impact on industrial structural steel (E410) by expired amiloride drug in 0.5 M solutions of HCl, H_2SO_4 and $NaHCO_3$. *Mor. J. Chem.* 9: 677-696. http://doi.org./10.48317/IMIST.PRSM/morjchem-v9i3.22346

Ugi, BU; Obeten, ME; Bassey, VM; Omaliko, EC; Obi, DN (2022). Adsorption and inhibition analysis of aconitine and tubocurarine alkaloids as eco-friendly inhibitors of pitting corrosion in

ASTM – A47 low carbon steel in HCl acid environment. *Indone. J. Chem.*, 22: 1 – 16. http://doi.org./10.22146/ijc.56745

Ugi, BU; Obeten, ME; Uwah, IE; Okafor, PC (2016) Aluminium corrosion abatement using non toxic and eco-friendly organic inhibitors. *J. Global Ecol. Environ*., 4(4): 242- 252

Ugi, BU; Omaliko, EC; Ikpi, ME (2024). Artequick as inhibitor of anodic site dissolutions in ASTM-A36 mild steel corrosion: computational and electrochemical approach, *Portugal. Electrochim. Acta., 42:* 155-171. https://doi.org/10.4152/pea.2024420301

Ugi, BU; Ugi, FB (2023). 817M40T Mild Steel Corrosion Remediation in 0.5 M Hydrochloric Acidic Environment Using Alkaloid and Flavonoid Extracts of Salvia Officinalis, *Phys. Chem. Res.*, 12: 121-133. http://doi.org./10.22036/pcr.2023.361046.2188

Ugi, BU; Uwah, IE; Okafor, PC (2016). Sulphuric acid corrosion of mild steel in leaves extract of Cnidoscolus aconitifolius plant. *J. Chem. Proc. Engr.* 46: 35 – 41

Uwah, IE; Ugi, BU; Ikeuba, AI; Essien, UB (2013). *Costusafer* Leave Extract as Nontoxic Corrosion Inhibitor in 5 M H_2SO_4 solution". *Global J. Pure Appl. Sci.*19 (2): 119 - 127.

Uwah, IE; Ugi, BU; Okafor, PC; Ikeuba, AI (2012). Investigation of the corrosion inhibition effects of Bitters on Mild Steel in acidic medium: A case study of *Andrographis paniculata* and *Vernonia amygdalina. Proceedings of the 35th Intl. Conf. Chem. Soc. Nig.* 2: 304 – 309.

Zaher, A; Chaouiki, A; Salghi, R (2020). Inhibition of mild steel corrosion in 1M hydrochloric medium by the methanolic extract of Ammi visnaga l. Lam seeds. *Hindawi Int. J. Corros.* 1: 1 – 10. http://doi.org./10.1155/2020/9764206